ITERATION THEORY (ECIT '02)
J. Sousa Ramos, D. Gronau, C. Mira,
L. Reich, A. Sharkovsky (Eds.)
Grazer Math. Ber., ISSN 1016–7692
Bericht Nr. 346 (2004), 137-156

A family of rational maps of the plane with prefocal set at infinity

Laura Gardini, Ilaria Foroni and Christian Mira

Abstract

The object of the present work is to study a *one-dimensional nonautonomous* equation (a *Mann iteration*) with geometric weights. Its study amounts to that of a *two-dimensional autonomous* rational map having a vanishing denominator in a non classical case. A map with a vanishing denominator possesses a set of points, called the *prefocal set*, with particular properties, that is, whose preimages are related to a single point called the *focal point*. A contact of a basin boundary with a prefocal set is a bifurcation giving rise to a qualitative change of this boundary by creation of *loops* at the focal point. With respect to classical cases, the particularity of the map family considered here consists in the fact that the prefocal set is at infinite distance, i.e. it is the set of points $(x, \pm\infty)$, x varying in $\Re$, the related focal points being at finite distance. The main result is related to the formulation of a one-to-one correspondence between arcs passing through the focal points and the points at infinity of type $(x, \pm\infty)$. A change of variables facilitates the study by relocating focal points and prefocal sets at finite distance.

1 Introduction

In several applications to economics the changes in discrete time (t) of the values taken by a state variable p_t (such as price or expected price, quantity, etc.) are described by the following "adaptive" mechanism, in which the new state p_{t+1} is a convex combination of the old state p_t and of the theoretical one $f(p_t)$:

$$p_{t+1} = (1 - y_t)p_t + y_t f(p_t) \tag{1}$$

where $f(x)$ is a continuous function representing the economic environment governing the changes. The weights depend on time as follows:

$$y_t = \frac{1}{\sum_{k=0}^{t} \rho^{t-k}} \tag{2}$$

Mathematics Subject Classification 2000: 37E99, 37G99.
Keywords and phrases: dynamical system, rational maps, focal points, prefocal sets.

with a *memory ratio* $\rho \in (0, 1)$, that is, we have an exponentially decreasing sequence y_t which depends on the terms of a geometric progression with *ratio* ρ ($y_0 = 1$, $y_1 = \frac{1}{1+\rho}$, $y_2 = \frac{1}{1+\rho+\rho^2}$, ...). The *one-dimensional nonautonomous* equation in (1) (which belongs to the class known also as *Mann iterations*) may be not easy to study.

In this paper we are not interested in the economic modelling and in the meaning of the state variables (the interested reader may refer to [Marimon (1997), Brock and Hommes (1997), Bischi and Gardini (2000), Foroni (2001)] and references therein), but in the mathematical formulation which may be used to study such a model. Noticing that the sequence of coefficients in (2) may be put in recursive form as $y_{t+1} = \frac{y_t}{y_t+\rho}$ assuming as initial condition $y_0 = 1$, (1) can be rewritten as follows:

$$\begin{aligned} p_{t+2} &= (1 - y_{t+1})p_{t+1} + y_{t+1} f(p_{t+1}) = \frac{\rho}{y_t + \rho} p_{t+1} + \frac{y_t}{y_t + \rho} f(p_{t+1}) \\ y_{t+1} &= \frac{y_t}{y_t + \rho} \end{aligned}$$

Now defining $x_t = p_{t+1}$ the original equation can be studied as a *two-dimensional autonomous* recurrence relationship

$$R_f : \begin{cases} x_{t+1} = \frac{\rho}{y_t+\rho} x_t + \frac{y_t}{y_t+\rho} f(x_t) \\ y_{t+1} = \frac{y_t}{y_t+\rho} \end{cases} \tag{3}$$

for which we are interested in the initial conditions (*i.c.* henceforth for short) $(x_0, y_0) = (f(p_0), 1)$, belonging to the line $y = 1$. In the applied context, when the state variable p_t represents an expected price, the first value p_1 is not taken as $f(p_0)$, but is assumed equal to p_0, in which case we shall consider as *i.c.* $(x_0, y_0) = (p_0, 1)$, i.e. a generic point on the line $y = 1$. Thus we are led to consider the family given by the *rational triangular maps* (3). As we shall see in the next section, the qualitative shape of the function $f(x)$ governs the dynamic behaviors of the so-called limiting map:

$$x_{t+1} = g_f(x_t) \quad , \quad g_f(x) = \rho x + (1 - \rho)\, f(x). \tag{4}$$

When the limiting function $g_f(x)$ is noninvertible its shape is not much relevant for the mathematical considerations associated with the properties of the map R_f**.** Thus the standard logistic function $f(x)$ will be essentially used as prototype**:**

$$f(x) = \mu x(1 - x), \quad \mu > 1. \tag{5}$$

With this choice of function $f(x)$, the map family R_f will be denoted by R. The families R_f and R are characterized by the existence of a vanishing denominator on the line $y = -\rho$. The equivalence of the models (1) and (3) (and the meaning of the model in the applied context) is restricted to the half-plane $y > 0$, and the *i.c.* on the line $y = 1$. Nevertheless we shall see in section 2 that in order to understand the dynamic behaviors, and bifurcations of basins, we have to study the dynamics of the family R_f also for $y < 0$**.**

The classical behavior of maps having a vanishing denominator is to posses a set of points, called the *prefocal set*, with particular properties, that is, whose preimages are related with particular points, called *focal points*. A contact of a basin boundary with a prefocal set is a bifurcation giving rise to a qualitative change of this boundary by creation of loops at a focal point and at its increasing rank preimages, as described in [Bischi and Gardini (1997)], [Bischi et al. (1999)] (see also [Bischi et al. (2001), (2003)]). In the present case, the family particularity consists in the fact that for R_f the prefocal set is located at infinite distance (with respect to the origin), being of type $(x, \pm\infty)$, x varying in $\Re$, the focal point being at finite distance. This situation gives rise to the occurrence of a sequence of bifurcations (as a function of the parameter μ) due to contacts of the basin boundary at infinity. This sequence of bifurcations leads to the basin fractalization. The main result is related to the formulation of a one-to-one correspondence between arcs passing through the *focal points* and the points at infinity of type $(x, \pm\infty)$. A change of variables will facilitate the study by relocating the *focal points* and the *prefocal set* at finite distance. These properties are shown in section 2, while an example is considered in section 3, where the complete characterization of the bifurcations is given. Section 4 deals with the sequence of bifurcations which is explained using the change of coordinate $y = \frac{1}{W}$. This leads to a rational map with focal points and prefocal sets at finite distance, already considered in [Bischi and Gardini (1997)].

2 Dynamics of the map R_f

This section is devoted to the dynamics study of the rational map given in (3), rewritten for convenience, by using the symbol " $'$ " to denote the unit time advancement operator, which gives the map:

$$R_f : \begin{cases} x' = \frac{\rho}{y+\rho}x + \frac{y}{y+\rho}f(x) \\ y' = \frac{y}{y+\rho} \end{cases} \tag{6}$$

This form is equivalent to the model in (1) when the *i.c.* are $(x_0, y_0) = (f(p_0), 1)$ or $(x_0, y_0) = (p_0, 1)$

The map R_f is not defined in the whole plane because the denominators of both components vanish on the line δ_S of equation

$$\delta_S : \qquad y = -\rho \tag{7}$$

Then R_f is well defined only if we exclude the singular line from the phase plane as well as its preimages of any rank. The preimages of δ_S belong to a sequence of lines located above δ_S, that is, in the strip $-\rho < y < 0$. In fact, it is easy to invert the second equation of R_f obtaining

$$y = \frac{y'\rho}{1-y'} \tag{8}$$

Then the points mapped by R_f on the singular line δ_S in one iteration are the points of

the line δ_S^{-1} of equation

$$\delta_S^{-1} : \qquad y = -\frac{\rho^2}{1+\rho} \tag{9}$$

located above δ_S. The points mapped on the singular line after n iterations of R_f belong to the line δ_S^{-n} of equation

$$\delta_S^{-n} : \qquad y = \frac{-\rho^{n+1}}{\sum_{k=0}^{n}\rho^k} = -\frac{\rho^{n+1}-\rho^{n+2}}{1-\rho^{n+1}}. \tag{10}$$

We remark that all these lines are located above δ_S, as the line $\delta_S^{-(n+1)}$ is higher than δ_S^{-n} for $n \geq 1$ and have the line $y = 0$ as the accumulation set when $n \to +\infty$. Thus the domain of definition of the map R_f is given by $E = \Re^2 \setminus \bigcup_{n=0}^{\infty} \delta_S^{-n}$.

The second component of R_f gives rise, starting from $y_0 = 1$, to a decreasing sequence of y_t values converging to $y^* = 1 - \rho$ as $t \to \infty$, i.e.

$$\lim_{t\to\infty} y_t = y^* = 1 - \rho$$

It results that the so called *limiting map* of R_f is the one-dimensional map $x' = g_f(x)$ given in (4), located on the line $y = y^*$, called the line of ω-limit sets. That is, the limiting map represents the restriction of R_f to the line $y = y^*$. Moreover, due to the second equation of the map R_f all the cycles belonging to the line of ω-limit sets are transversely attracting.

As the map R_f has a vanishing denominator in the points of the line $y = -\rho$, it follows that focal points (if they exist) must necessarily belong to it. On $y = -\rho$ the numerator in the first component of R_f becomes $\rho(x - f(x))$, thus it vanishes if and only if $f(x) = x$, that is, at each fixed point of the function f and also of the limiting map g_f. It follows that the first component of R_f takes the form $0/0$ in the points $Q = (z^*, -\rho)$ where z^* is a fixed point of the limiting map $g_f(x)$. It is easy to see that the points of type $Q = (z^*, -\rho)$ are not the classical focal points met in the papers referenced above. Indeed, although the first component of R_f takes finite values on different arcs crossing these points (in a small neighborhood of them), the second component of R_f is not bounded, so that we get points in a neighborhood of points of type $(x, \pm\infty)$. This is due to the presence of the same denominator in the second component of R_f, without cancellation of the numerator. Thus for the family R_f the points which usually constitute the prefocal set are now at infinity, being of type $(x, \pm\infty)$. However as for the focal points described in the papers [Bischi and Gardini (1997)] and [Bischi et al. (1999)], a one-to-one correspondence can be established between the slopes of arcs passing through a focal point Q and the points at infinity $(x, \pm\infty)$. Indeed consider an arc γ transverse to δ_S in a point $Q = (z^*, -\rho)$, represented in parametric form by

$$\gamma(\tau) : \begin{cases} x(\tau) = z^* + \xi_1\tau + \xi_2\tau^2 + ... \\ y(\tau) = -\rho + \eta_1\tau + \eta_2\tau^2 + ... \end{cases} \qquad \tau \neq 0 \tag{11}$$

To study the shape of the set $R_f(\gamma)$, let us assume that γ is deprived of the point $(z^*, -\rho)$, so that the arc can be considered as the union of two disjoint pieces, say $\gamma = \gamma_+ \cup \gamma_-$, where γ_- and γ_+ are obtained from (11) with $\tau < 0$ and $\tau > 0$ respectively. Considering the image $R_f(\gamma)$ we have

$$\lim_{\tau \to 0\pm} R_f(\gamma(\tau)) = (z^* + \rho \frac{\xi_1}{\eta_1}[(1 - f\,'(z^*)], \mp\infty) \tag{12}$$

where

$$f\,'(x) = \frac{df}{dx}(x)$$

Thus $R_f(\gamma)$ is made up of two unbounded arcs, located on opposite side of the phase plane, issuing from the point (12). Let $m = \dfrac{\eta_1}{\xi_1}$ be the slope of the tangent to the arc γ in the point $Q = (z^*, -\rho)$, we may write

$$\lim_{\tau \to 0\pm} R_f(\gamma(\tau)) = (u_m, \mp\infty), \quad \text{with} \quad u_m = z^* + \rho \frac{1 - f\,'(z^*)}{m} \tag{13}$$

See the qualitative picture in Figure 1a. As m varies in $\Re\backslash\{0\}$ we obtain all the points of type $(x, \pm\infty)$. Thus the classical definition, reminded in the introduction (also cf. [Bischi and Gardini (1997)] and in [Bischi et al. (1999), (2003)]) for maps T having a vanishing denominator only in one of the components, can easily be extended to the family R_f. This family has the particularity that the two components defining R_f have the same vanishing denominator, the second one having a non cancelling numerator at a point Q, which leads the image of a point in a neighborhood of Q to be in a neighborhood of the point $(x, \pm\infty)$. In this sense the points Q (each one associated with any fixed point of $f(x)$) are singular focal points of R_f. Arcs crossing through $Q = (z^*, -\rho)$ with a slope m are mapped by R_f into two unbounded arcs which cross the point at infinity $(u_m, \mp\infty)$, where u_m is given in (13) with the suitable value of z^* (Figure 1a). It results that the prefocal set is the set of points $(u, \mp\infty)$, u varying in $\Re$. A consequence is that the points Q may be crossed by infinitely many invariant phase curves (in particular arcs of basin boundary) which also cross points at infinity, of type $(u_m, \mp\infty)$. This characteristic has a particular importance in explaining the bifurcations occurring in the basins generated by the family R_f.

The points $(u, \mp\infty)$ constitute a singular prefocal set, however, as in the classical case, the relation given in (13) can be inverted, that is, an arc issuing from a point $(u, \mp\infty)$ is mapped by R_f^{-1} into arcs issuing from the *focal points* $Q = (z^*, -\rho)$ with tangents in such points having slopes

$$m_u = \frac{\rho}{u - z^*}[1 - f\,'(z^*)] \tag{14}$$

The relation (8) shows that as y' tends to $\mp\infty$ we have $y \to -\rho$. Writing the first relation of (3) as $x' = x + y'[f(x) - x]$, given some x', as $y' \to \mp\infty$ a finite value of x may be obtained only if it satisfies $f(x) = x$, and thus only at a fixed point x^* of $f(x)$, and

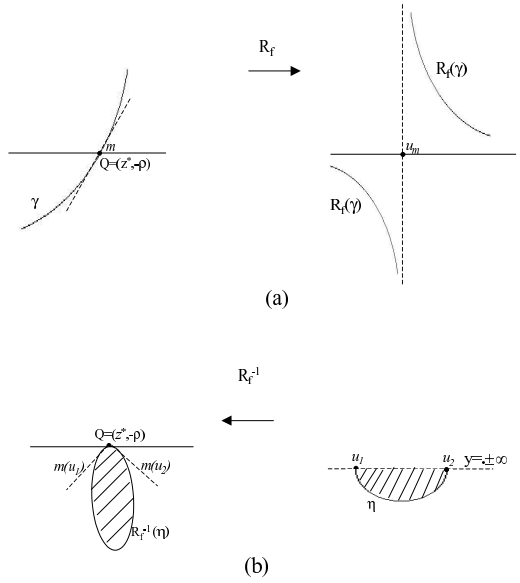

Figure 1: (a) Qualitative figure representing the image of an arc through a *focal point* Q for the map R_f. (b) Qualitative figure representing the preimage of an arc through the points $(u_i, \pm\infty)$ for the map R_f.

thus of $g_f(x)$. It follows that the preimage of an arc crossing through $y' \to \mp\infty$ gives loops issuing from the focal points, so that it may give rise to *lobes* in the basins, as qualitatively shown in Figure 1b.

We note that when $f(x)$ has k fixed points z_i^*, then $g_f(x)$ has k fixed points z_i^*, then R_f has k *focal points* $Q_i = (z_i^*, -\rho)$, and k distinct inverses of R_f exist, as seen in the example of the next section.

3 Basin bifurcations of the map R

The basins generated by the map R undergo a sequence of bifurcations described in this section. Let us first recall that in the chosen example for f the limiting map we obtain on the line of ω-limit set $y = y^* = 1 - \rho$ is:

$$x' = g(x) \quad , \quad g(x) = \rho x + (1 - \rho)\,\mu x(1 - x) \tag{15}$$

This map is topologically conjugate to the Myrberg's map $v' = v^2 - \lambda$ (studied in detail in the books [Gumowski and Mira (1980)] and in [Mira (1987)]). This appears from a linear change of variable $x = \alpha v + \beta$, giving $\lambda = b^2 - b$, $b = [\rho + (1-\rho)\,\mu]/2$, $a\alpha = 1$, $a\beta = -b$, $a = -(1-\rho)\,\mu$. The inverse relation $\mu = h(\lambda, \rho)$ for $\mu > 0$ is

$$\mu = 1 + \sqrt{1 - \frac{\rho^2 - 2\rho - 4\lambda}{(1-\rho)^2}}$$

As $g(x)$ has two fixed points ($s^* = 0$ and $x^* = 1 - \frac{1}{\mu}$), also for the family R we have two related fixed points: $S^* = (s^*, y^*) = (0, 1-\rho)$ and $P^* = (x^*, y^*) = (1 - \frac{1}{\mu}, 1-\rho)$. Besides S^* and P^*, also the points $y = 0$ of the x-axis are fixed points of the map R. From the Jacobian matrix of R it appears that the fixed points on $y = 0$ are transversely repelling. As already noticed, from the second component defining R it is clear that all the attracting sets belong to the line of ω-limit sets $y = y^*$. The fixed points and cycles on this line are always transversely attracting. In particular, the points of the domain of definition of the map belonging to the vertical line through each fixed point (z_i^*, y^*), are on the stable set of such a point (i.e. except for the points on the lines δ_S^{-n}, $n \geq 0$, the vertical line belongs to the stable set).

Regarding the map R, for $\mu > 1$ S^* is a saddle**.** Let ρ be $\rho = 0.75$. A fractal bifurcation structure of "*box-within-a-box*" type, (also said of "*embedded boxes*" type in [Gumowski and Mira (1980)] and [Mira (1987)]), takes place in the interval $-1/4 \leq \lambda \leq \lambda_1^* = 2$, i.e. $1 \leq \mu \leq \mu_1^* = 13$, where R has only one attractor at finite distance. This attractor is the fixed point P^*, stable when $-1/4 < \lambda \leq 3/4$, $\lambda = b^2 - b$, $b = [\rho + (1-\rho)\,\mu]/2$, i.e. for $1 < \mu < 9$. It undergoes a flip bifurcation for $b = 3$ giving rise to a stable period two cycle in the interval $3/4 < \lambda < 5/4$, i.e. for $9 < \mu < 10.79795897....$ Inside the interval $-1/4 < \lambda \leq \lambda_{1s} \simeq 1.401155189$, i.e.$1 < \mu < \mu_{1s} \simeq 11.27978269$, occurs a period doubling cascade from P^*. When λ, or μ, increases in the interval $\lambda_{1s} \leq \lambda \leq \lambda_1^* = 2$, i.e. $\mu_{1s} \leq \mu \leq \widetilde{\mu_1^*} = 13$, infinitely many sequences made up of infinitely many unstable cycles (generating a *strange repeller*) are generated on the segment $0 < x < [\rho + (1-\rho)\mu]/[(1-\rho)\mu]$, of the line $y = 1 - \rho$. This strange repeller coexists with a period k stable cycle, $k = 3, 4, 5, ...$, giving rise to a *chaotic transient* toward such an attracting set, or an attractor made up of cyclical chaotic intervals exists. For $\mu \geq \widetilde{\mu_1^*} = 13$ all the possible cycles have been created on $y = 1 - \rho$, and they are all unstable.

As seen above, the stable sets of the fixed points on the line of ω-limit set $y = 1 - \rho$ cross through the *focal points* which are associated with the fixed points. So in the case of (15) two focal points exist, given by:

$$Q_1 = (0, -\rho)\ ,\ Q_2 = (1 - \frac{1}{\mu}, -\rho)$$

Differently from the study of the attracting sets (which are those of the limiting one-dimensional map g on the line of ω-limit sets $y = y^* = 1 - \rho$), the basins study implies the consideration of R in the whole plane. It is worth noting that the restriction of the

basins of R to the line of *i.c.* $y = 1$ gives the basins for the original model (1), i.e. the one-dimensional nonautonomous equation. The fixed point S^* is always a saddle When $1 < \mu < 9$, P^* is an attracting node. For the map g, i.e. on the line $y = y^*$, the basin of P^* is the interval $]0, g^{-1}(0)[$, being $g^{-1}(0)$ the rank-1 preimage of the saddle origin distinct from itself, here $g^{-1}(0) = [\rho + (1-\rho)\mu]/[(1-\rho)\mu]$. The points of the intervals $]-\infty, 0[$ and $]g^{-1}(0), +\infty[$ have divergent trajectories. This domain of divergence is denoted by $B(\infty)$. The basin of the fixed point P^*, $B\,(P^*)$, is separated from the set of points having divergent trajectories, $B(\infty)$, by the same frontier, say $\mathcal{F}$, $\mathcal{F} = \partial B(\infty)$. In our case, $\mathcal{F}$ consists of the closure of stable set of the saddle S^*, that is, $\mathcal{F} = \overline{W^S(S^*)}$. The local stable set of S^* clearly belongs to the $y-$axis ($x = 0$), in fact all the points of the $y-$axis ($x = 0$), except for the origin O and the points on the lines δ_S^{-n}, belong to the stable set $W^S(S^*)$. Thus the whole $y-$axis, denoted by ω_0 for short, belongs to the frontier $\mathcal{F}$ (see Figure 2). Let $R^{-n}(x, y)$ be the set of all the rank$-n$ preimages of a point (x, y). Then:

$$\mathcal{F} = \overline{W^S(S^*)} = \bigcup_{n \geq 0} \omega_{-n}, \quad \omega_{-n} = R^{-n}(\omega_0), \quad \omega_0 = \{x = 0\} \tag{16}$$

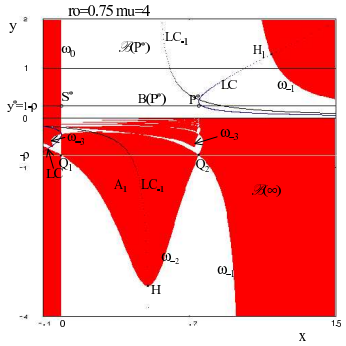

Figure 2: Basins of attraction of the map R for $\mu = 4 < \mu_0^* = 4.64575$.

In Figure 2 the fixed points P^* and S^* are shown on the line of ω-limit sets $y = y^* = 1-\rho$, the basin $B\,(P^*)$ is white, while the basin $B(\infty)$ is the one in grey. For the original model (1) the basin is denoted $\mathcal{B}\,(P^*)$, that is, $\mathcal{B}\,(P^*) = B\,(P^*) \cap \{y = 1\}$. The map R is a noninvertible map of $(Z_0 - Z_2)$ type, i.e. the plane is made up of the closure of two regions: Z_0 each point of which has no real preimage, Z_2 each point of which has two real rank-one preimages. A point (x', y') of the plane either has no rank-1 preimages,

or two preimages, given by $R^{-1}(x',W') = R_1^{-1}(x',W') \cup R_2^{-1}(x',W')$, where

$$R_{1,2}^{-1}: \begin{cases} x = \dfrac{[1-y'(1-\mu)] \pm \sqrt{\Delta}}{2y'\mu}, & \Delta = [y'(1-\mu)-1]^2 - 4\mu x' y' \\ y = \dfrac{y'\rho}{1-y'} \end{cases} \tag{17}$$

constitute the inverses of the map R. The open region Z_2 is defined by $\Delta(x',y') > 0$, the open region Z_0 is defined by $\Delta(x',y') < 0$. These two regions are separated by the critical curve LC (from the french "Ligne Critique" [Gumowski and Mira (1980)], see also [Mira et al. (1996)]), given by the points for which $\Delta = 0$, that is:

$$LC = \{(x,y) \mid [y(1-\mu)-1]^2 - 4\mu x y = 0\}. \tag{18}$$

The points belonging to LC have two merging rank-1 preimages (obtained from $R_{1,2}^{-1}$ with $\Delta = 0$) located on the set LC_{-1} in which the Jacobian determinant vanishes:

$$LC_{-1} = \{(x,y) \mid 2\mu x y - \rho - \mu y = 0\} \tag{19}$$

The set LC_{-1} is the hyperbola $y = \frac{\rho}{\mu(2x-1)}$, with vertical asymptote in the line $x = 0.5$. Of course $LC = T(LC_{-1})$ and, since LC_{-1} is made up of two unbounded branches, also LC is formed by two unbounded branches (see Figure 2). The knowledge of the curves LC and LC_{-1} is important in the determination of the preimages of the local stable set of S^*, according to (16).

From (17) the rank-1 preimages of ω_0 (the line $x = 0$) can be easily defined. It is an hyperbola denoted by ω_{-1}, $\omega_{-1} = R^{-1}(\omega_0)$, of equation

$$\omega_{-1} \quad : \quad y = \frac{\rho}{\mu(x-1)}$$

In Figure 2 we can see that ω_{-1} intersects the prefocal set in the points $(1;\pm\infty)$, and the upper branch of ω_{-1} intersects LC in a point H_1. The preimage of ω_{-1}, $\omega_{-2} = R^{-1}(\omega_{-1}) = R^{-2}(\omega_0)$, includes two arcs issuing from the point H belonging to LC_{-1} and crossing the two focal points Q_1 and Q_2. At the focal points $Q_1(0,-\rho)$ and $Q_2(1-\frac{1}{\mu},-\rho)$, according to (14) with $u = 1$, $z^* = 0$ and $z^* = 1-\frac{1}{\mu}$, these arcs $\widehat{Q_1H}$ and $\widehat{Q_2H}$ have the slopes:

$$m(Q_1) = \rho(1-\mu) < 0, \qquad m(Q_2) = \rho\mu(\mu-1) > 0.$$

Let $A_1 \subset (y < -\rho)$ be the area of $B(\infty)$ bounded by the arcs $\widehat{Q_1Q_2}$, $\widehat{Q_1H}$ and $\widehat{Q_2H}$. As μ increases, the minimum of the arc $\widehat{Q_1H} \cup \widehat{Q_2H}$ has its ordinate which tends towards $y = -\infty$ (see the point H in Figure 2). It results a contact with the prefocal set (at infinity) at a bifurcation value $\mu = \mu_0^*$. For $\mu < \mu_0^*$ two small arcs of ω_{-3} approach the focal points Q_1 and Q_2 (Figure 3a). When $\mu = \mu_0^*$ these two arcs have a cusp contact with Q_1 and Q_2. When $\mu = \mu_0^* + \varepsilon$, $\varepsilon > 0$ being sufficiently small, a lobe (Bischi et al. [1999)]) of $\partial B(\infty)$ is created at each of the focal points Q_1 and Q_2 (Figure 3b).

Figure 3b shows the strip $-\rho < y < 0$ which contains the set of non definition of the map R, i.e. $\cup_{n\geq 0}\delta_S^{-n}$ given by (10), $\delta_S^{-0} \equiv \delta_S$. The exact bifurcation value is given by

$$\mu_0^* = 2 + 2\sqrt{1+\rho} \tag{20}$$

as it will be explained below.

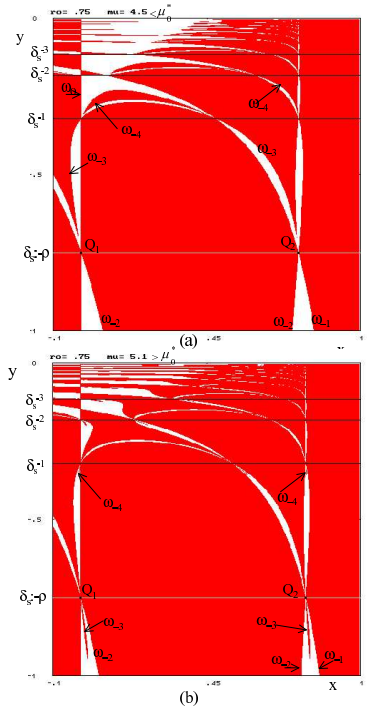

Figure 3: Basins of attraction of the map R. For $\mu = 4.5 < \mu_0^* = 4.64575$ in (a), for $\mu = 5.1 > \mu_0^*$ in (b).

After the crossing through $y' \to \mp\infty$, for $\mu = \mu_0^* + \varepsilon$, $\varepsilon > 0$, the arc $\widehat{Q_1H} \cup \widehat{Q_2H}$ creates a new area A_2 of $B(\infty)$ in the region $y > 0$, continuation of A_1. The area A_2 tends toward $y = +\infty$ when $\varepsilon \to 0$ (see Figure 4). The two rank-1 preimages of A_2 are the two lobes bounded by arcs of ω_{-3} issuing from the focal points Q_1 and Q_2. Then with increasing values of μ the following behavior occurs:

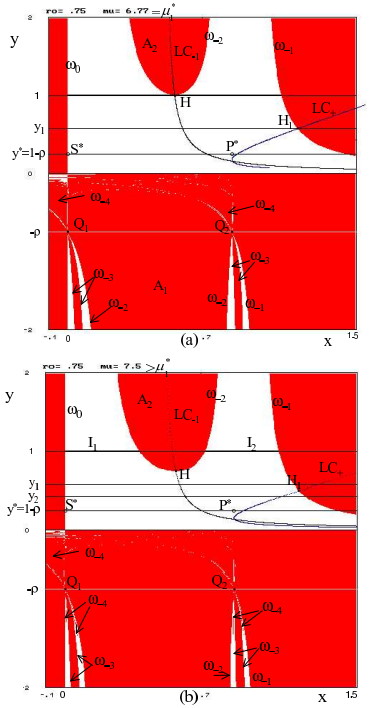

Figure 4: Basins of attraction of the map R. In (a) for $\mu = 6.773369 = \mu_1^*$, for $\mu = 7.5 > \mu_1^*$ in (b).

- The ordinate of the minimum of each lobes bounded by ω_{-3} tends toward $y = -\infty$ and a new contact at infinity occurs at the bifurcation value μ_1^*,

$$\mu_1^* = 2 + \rho + 2\sqrt{(1+\rho)\,(1+\rho+\rho^2)} \tag{21}$$

- 2^2 arcs of ω_{-4} have cusps in the focal points preparing the creation of four new lobes issuing from them,

- for $\mu = \mu_1^*$ the first bifurcation of the basin $B\,(P^*)$ $(\rho = 0.75)$ occurs because the portion A_2 (of the basin $B(\infty)$) reaches (from above) the line of initial conditions $y = 1$ (see Figure 4a), and after the bifurcation the basin $B\,(P^*)$ will be made up of 2^1 intervals.

Consider the point $H \in LC_{-1} \cap \omega_{-2}$ at the minimum of the boundary of A_2. The bifurcation $\mu = \mu_1^*$ is characterized by $H \in \{y = 1\}$ or, equivalently, by $y(H_1) = y_1 = \frac{1}{1+\rho}$, where $H_1 = \omega_{-1} \cap LC_+$, LC_+ being the branch of LC belonging to the half-plane $y > 0$. This condition allows to determine the bifurcation value given in (21). We can also understand that the bifurcation value $\mu = \mu_0^*$ occurs when the point H has $y = \infty$ and $H_1 \in \{y = 1\}$, condition which allows us to determine the first bifurcation value given in (20).

For $\mu > \mu_1^*$, 2^2 lobes bounded by arcs of ω_{-4} are created through the focal points. The two lobes bounded by ω_{-3} cross through $y = \pm\infty$ and continue their development turning into two tongues in the region $y > 0$, their minimum decreasing when μ increases. They reach the line $y = 1$ (of initial conditions) when $y(H) = y_1 = \frac{1}{1+\rho}$ and $y(H_1) = y_2 = \frac{1}{1+\rho+\rho^2}$ (see Figure 5a). This condition permits to determine the bifurcation value

$$\mu_2^* = 1 + \frac{1}{1+\rho+\rho^2} + 2\sqrt{\frac{1}{1+\rho+\rho^2}\left(1 + \frac{\rho}{1+\rho+\rho^2}\right)}$$

For $\mu = \mu_2^*$ the 2^2 lobes of ω_{-4} have a contact with at $y = -\infty$, and 2^3 arcs of ω_{-5} have cusps in the focal points preparing the creation of eight new lobes issuing from them. For $\mu > \mu_2^*$ the 2^2 lobes continue their development turning into two tongues in the region $y > 0$, their minimum decreasing when μ increases (see Figure 5b). And so on, infinitely many contact bifurcations occur with infinity, at $y = \pm\infty$, and thus with the line $y = 1$ (line of initial conditions for (1)). Bifurcation values $\mu = \mu_k^*$ $(k \in N)$ occur when new tongues coming from $y = +\infty$ reach the line $y = 1$. For these values, the lobes bounded by arcs of $\omega_{-k-1} = T^{-k-1}(\omega_0)$ become tangent to the line $y = 1$, and $y(H_1) = y_k = \frac{1}{1+\ldots+\rho^k}$, condition which allows to determine all the bifurcation values, that is:

$$\mu_k^* = \frac{1 + y_k + 2\sqrt{y_k + \rho}}{y_k} \quad , \quad y_k = 1/\sum_{j=0}^{k} \rho^k \quad \text{for} \quad k \geq 0$$

It is clear that as μ increases also the attracting sets of the limiting map g modifies according to the rules of the fractal bifurcation structure of box-within-a-box type mentioned above. So one has to deal with other attracting sets, say A, at finite distance (cycles or cyclic chaotic intervals). As long as P^* remains stable $(1 < \mu \leq 9)$ $\partial B(P^*) = \partial B(\infty)$. For $9 < \mu < \mu_{1s}$, $\partial B(A) \neq \partial B(\infty)$, being A the attracting set, and $\partial B(A)$ is not fractal including the stable set of the period 2^i, $i = 1, 2, 3, ...$, saddle cycles born in this interval. Increasing μ, the bifurcations generated by the one-dimensional map $x' = g(x)$ are those described at the beginning of this section. Remind that for $\mu_{1s} \leq \mu \leq \mu_1^* = 13$, the segment $0 < x < [\rho + (1-\rho)\mu]/[(1-\rho)\mu]$ of the line $y = 1 - \rho$ contains a *strange repeller* SR, i.e. a repulsive fractal set constituted by infinitely many sequences made up of infinitely many unstable cycles generated by the box-within-a-box bifurcation structure. For the two-dimensional map R these cycles are saddles, and their stable set belong to the white region in Figure 6. Then $\partial B(A) \neq \partial B(\infty)$, but $\partial B(A)$ is

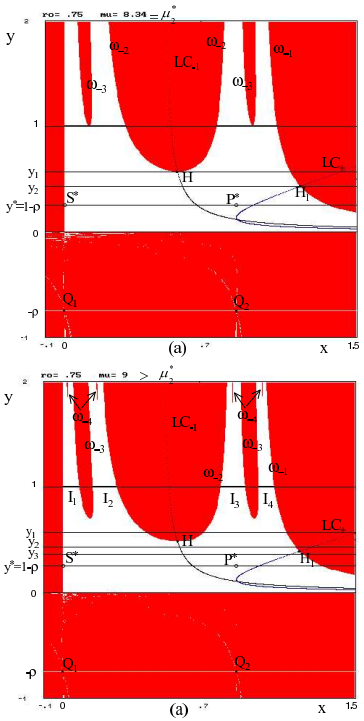

Figure 5: Basins of attraction of the map R. In (a) for $\mu = 8.3417115 = \mu_2^*$, for $\mu = 9 > \mu_2^*$ in (b).

fractal including the stable set $W^s(SR)$ of SR, $B(A)$ being not fractal The basin boundary $\mathcal{F} = \partial B(\infty)$ becomes more and more complex in the interval $\mu_{1s} \leq \mu \leq \widetilde{\mu_1^*} = 13$, but not fractal because the number of lobes remains finite, according to the nature of the bifurcations $\mu = \mu_k^*$. For $\mu_{1s} \leq \mu \leq \widetilde{\mu_1^*}$, the attractor is either a period k stable cycle, $k = 3, 4, 5, ...$,or consists of cyclical chaotic intervals. In the plane region containing $W^s(SR)$ (for example the white region in Figure 6) a chaotic transient (in the x direction) toward the attractor occurs. Figure 6a shows the basin situation at the bifurcation value μ_3^*. When μ increases inside $\mu_{1s} \leq \mu \leq \widetilde{\mu_1^*}$, due to the addition of new infinite sequences of infinitely many saddle cycles, the fractalization of SR increases with that of the basin boundary $\partial B(A)$ (but $B(A)$ is not fractal). Figure 6b represents the basin $B(\infty)$ when $\rho = 0.75$ and $\mu = 12.342$, parameter values giving a stable period three node cycle on the line $y = 1 - \rho$.

When μ reaches the limiting value

$$\mu_\infty^* = \lim_{k\to\infty} \mu_k^* = \frac{4-\rho}{1-\rho} \tag{22}$$

the point H_1, together with all its infinite preimages, located at the tongues extremities,

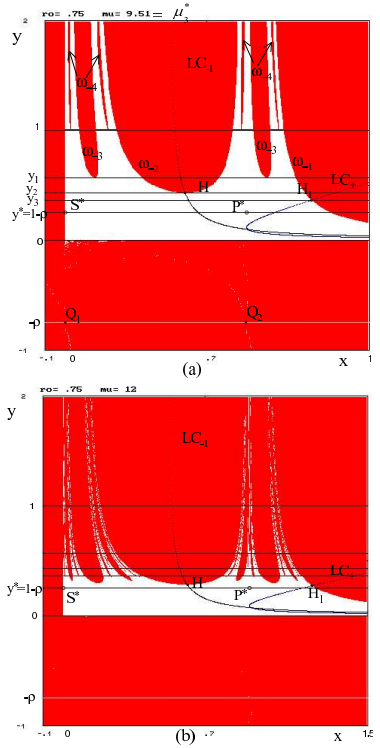

Figure 6: Basins of attraction of the map R. In (a) for $\mu = 9.5108 = \mu_3^*$, for $\mu = 12$ in (b).

reach the line of the ω-limit sets $y = y^* = 1-\rho$. Thus at $\mu = \mu_\infty^*$ infinitely many lobes of $B(\infty)$ have been created, and all have a contact with a chaotic attractor $\mathcal{A}$ located on the line $y = y^*$. This contact between $\partial B(\infty)$ and the chaotic set causes the disappearance of $\mathcal{A}$ and for $\mu > \mu_\infty^*$ the generic trajectory of the map R is divergent. It is worth noting that for $\mu = \mu_\infty^*$, the corresponding value of λ in the Myrberg's map, $v' = v^2 - \lambda$,

$\lambda = b^2 - b$, $b = [\rho + (1-\rho)\,\mu]/2$, is such that $\lambda = \lambda_1^* = 2$ (limit of existence of an attractor on $y = 1-\rho$), i.e. does not depends on ρ.

We also remark that our Figs. 2-6 do not use a fixed value of the parameter ρ, nevertheless the global analysis of the basin boundaries described in this section holds for any value of the parameter ρ belonging to the interval $(0, 1)$.

We end this section observing that we can equivalently study the family R_f, which represents the model in (1), by using a change of variable, as we shall see in the next section. However the results observed with the map R are important not only in an applied context of the model (which can be obtained also in section 4) but mainly for the mathematical properties of the particular focal points associated with a prefocal sets at infinity, as already observed in [Foroni 2001]. Such singularities play the same important role, as that of the focal points with prefocal set at finite distance.

4 An alternative study

The peculiarities of the family R_f seen in the previous sections may be associated with the peculiarities of another family of maps, obtained from it by using the change of variable $y = \frac{1}{W}$. In fact, in such a case we get a two-dimensional rational family, representing the original model (1) when the *i.c.* are $(x_0, W_0) = (f(p_0), 1)$, or $(x_0, W_0) = (p_0, 1)$:

$$T_f : \begin{cases} x' = \dfrac{\rho W}{1+\rho W} x + \dfrac{1}{1+\rho W} f(x) \\ W' = 1 + \rho W \end{cases} . \tag{23}$$

This family T_f has standard focal points with prefocal lines at finite distance, and so the bifurcation mechanism is easier to study because all the contact bifurcations occur at finite distance. When we consider in particular for $f(x)$ the logistic function then we have the map T:

$$T : \begin{cases} x' = \dfrac{\rho W}{1+\rho W} x + \dfrac{\mu x(1-x)}{1+\rho W} \\ W' = 1 + \rho W \end{cases} \tag{24}$$

For the map T_f, the state variable W, whose *i.c.* of interest is 1, gives now an increasing geometric sequence ($W_0 = 1$, $W_1 = 1+\rho$, $W_2 = 1+\rho+\rho^2$, ...), converging to $\frac{1}{1-\rho}$. The line of ω-limit sets is thus $W = W^* = \frac{1}{1-\rho}$, on which the limiting map (which governs the asymptotic behavior) is always the same function $g_f(x)$ given in (4). Figures 7 and 8 represent the basins of the map T (light grey points converge to the attracting set at finite distance, while dark grey points give divergent trajectories as in the previous section). Clearly the basins are similar (having the same restriction on the related lines of ω-limit sets), but now a better explanation of the bifurcation mechanism can be given. In fact, the dynamic properties of the family of maps T_f in (23) has been the object of the paper by [Bischi and Gardini (1997)], see also [Bischi and Gardini (1999) and Bischi *et al.* (1999)], where the properties related to the focal points and prefocal sets have been described. The particular case $f(x) = \mu x(1-x)$, i.e. the map T in (24), has

not been considered explicitly in that references, but this has been done in [Bischi and Gardini (2000)] and we shall briefly recall here the results.

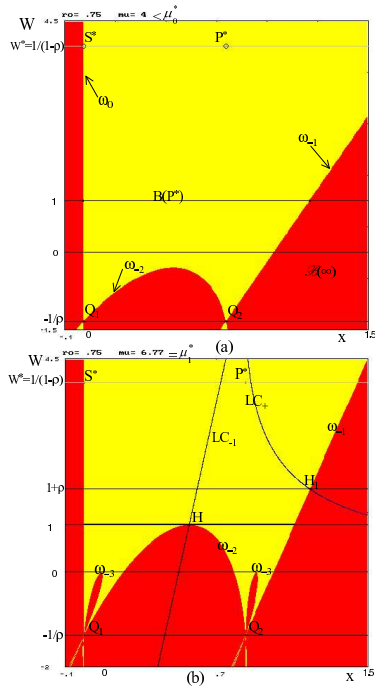

Figure 7: Basins of attraction of the map T. In (a) for $\mu = 4 < \mu_0^*$, for $\mu = 6.773369 = \mu_1^*$ in (b).

The singular line δ_s in which the denominator of the first equation of T vanishes is $W = -\frac{1}{\rho}$ which includes the two focal points

$$Q_1 = \left(0, -\frac{1}{\rho}\right) \quad \text{and} \quad Q_2 = \left(1 - \frac{1}{\mu}, -\frac{1}{\rho}\right). \tag{25}$$

associated with the fixed points of T : $S^* = (s^*, W^*) = (0, \frac{1}{1-\rho})$ and $P^* = (x^*, W^*) = (1 - \frac{1}{\mu}, \frac{1}{1-\rho})$, and T has no other fixed points. The prefocal set associated with both the focal points is the line δ_Q of equation $W = 0$ (*i.e.* the $x-$axis).

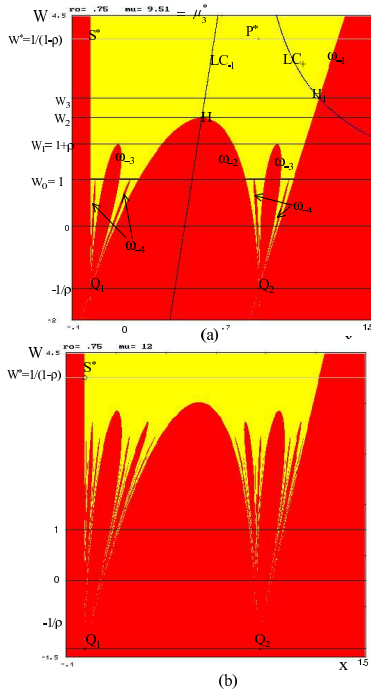

Figure 8: Basins of attraction of the map T. In (a) for $\mu = 9.5108 = \mu_3^*$, for $\mu = 12$ in (b).

As in the previous section, for $\mu > 1$ the boundary of the basin of divergent trajectories, $\mathcal{F} = \partial B(\infty)$, is given by the closure of the stable set of the saddle S^*

$$\mathcal{F} = \overline{W^S(S^*)} = \bigcup_{n\geq 0} \omega_{-n}, \quad \omega_{-n} = T^{-n}(\omega_0), \quad \omega_0 = \{x = 0\} \tag{26}$$

where we have denoted by ω_0 the $W-$axis, and $T^{-n}(x, W)$ denotes the set of all the rank$-n$ preimages of the point (x, W). In our case, the map (24) is a noninvertible map of $Z_0 - Z_2$ type, i.e. a point (x', W') has no rank-1 preimages or two preimages, given by $T^{-1}(x', W') = T_1^{-1}(x', W') \cup T_2^{-1}(x', W')$, where

$$T_{1,2}^{-1} : \begin{cases} x = & \frac{((W'+\mu-1)\pm\sqrt{(W'+\mu-1)^2-4\mu x'W'}}{2\mu} \\ W = & \frac{W'-1}{\rho} \end{cases} \tag{27}$$

$\Delta(x, W) = (W' + \mu - 1)^2 - 4\mu x' W' > 0$ denotes the region Z_2, while Z_0 is given by $\Delta(x, W) < 0$. These two regions are separated by the critical curve LC :

$$LC = \left\{(x, W) \mid \Delta(x, W) = (W + \mu - 1)^2 - 4\mu x W = 0\right\} \tag{28}$$

whose points have two coincident preimages located on LC_{-1}, given by the straight line of equation

$$LC_{-1} = \{(x, W) \mid \rho W - 2\mu x + \mu = 0\}. \tag{29}$$

From (27) the rank-1 preimages of ω_0 (the line $x = 0$) can be easily computed, it is the line of equation:

$$\omega_{-1} \quad : \quad W = \frac{\mu}{\rho}(x - 1) \tag{30}$$

(see Figs. 7,8). It can be noticed that ω_{-1} "crosses" the singular line through the focal point Q_2. The portion of this line located below the critical curve LC belongs to the region Z_2, hence it has two preimages, say ω_{-2}^1 and ω_{-2}^2, whose equation can be obtained from (27) with $W' = \frac{\mu}{\rho}(x' - 1)$. These two preimages are located at opposite sides with respect to the line LC_{-1} and merge in the point H, given by the merging preimages of the point $H_1 = \omega_{-1} \cap LC_+$, where LC_+ denotes the upper branch of LC (see Figure 7b and Figure 8a). After some computations it is possible to see that such preimages belong to the curve of equation:

$$\omega_{-2} \quad : \quad x = \frac{\mu + \rho W \pm \sqrt{(\mu + \rho W)^2 - 4(1 + \rho W)(\mu + \rho + \rho^2 W)}}{2\mu}. \tag{31}$$

The locus ω_{-2} (31) represents an hyperbola if $\rho < \frac{1}{4}$, a parabola if $\rho = \frac{1}{4}$, an ellipse if $\rho > \frac{1}{4}$ (as in Figs. 7,8, obtained with $\rho = .75$), and crosses the line of non definition $W = -1/\rho$ at the focal points.

It is clear that now all the contact bifurcations occur at finite distance, when the point $H_1 = \omega_{-1} \cap LC_+$ belongs to the line $W = W_k = 1 + \rho + ... + \rho^k$, and the bifurcation values $\mu = \mu_k^*$ are given explicitly by

$$\mu_k^* = 1 + W_k + 2\sqrt{W_k(1 + \rho W_k)} \ , \ W_k = 1 + \rho + ... + \rho^k = \frac{1 - \rho^{k+1}}{1 - \rho} \ , \ k \geq 0. \tag{32}$$

At $\mu = \mu_k^*$ for $k \geq 1$ the arcs of $\omega_{-k-1} = T^{-k-1}(\omega_0)$ become tangent to the line of initial conditions. This implies that the number of lobes of $B(\infty)$ is doubled and 2^{k-1} new holes are created on the basin $B(A)$ belonging to the line of *i.c.*, and the basin becomes made up of 2^k intervals. The whole sequence of bifurcations causes a fractalization of the basin boundaries near the focal points that gives a "finger-shaped" structure of $B(\infty)$.

5 Conclusions

This paper has considered the one-dimensional nonautonomous equation known as *Mann iteration* (given in (1)) with a particular type of coefficients (a geometric sequence). It often occurs in applied contexts (as for example in economic studies). We have seen that its study may be reduced to that of a two-dimensional autonomous system, that is to the map R_f (or to the map T_f). The initial conditions must be taken on the line $y = 1$ (or on the line $W = 1$). The states of the nonautonomous equation belong to the lines $y = y_k = \frac{1}{1+\rho+...+\rho^k}$ (or $W = W_k = 1 + \rho + ... + \rho^k$) and their ω-limit sets are those of the limiting map $g_f(x)$ on the line $y = y^* = 1 - \rho$ (or $W = W^* = \frac{1}{1-\rho}$). The basins of the attracting sets for the nonautonomous equation are those on the line of *i.c.*. Examples have been given taking the logistic function as prototype of a one-dimensional noninvertible map $f(x)$.

While the family of maps T_f is of standard type in the class of maps with a vanishing denominator, the family R_f is nonstandard. In fact, although the *focal points* are at finite distance, the related *prefocal set* is at infinity, it is the set of points $(x, \pm\infty)$, x varying in $\Re$. This gives rise to particular contact bifurcations between the basin boundary $\mathcal{F} = \partial B(\infty)$ and infinity, which lead to the creation of *lobes* through the focal points. However we have seen that also in this case a one-to-one correspondence between arcs passing through the focal points and through points at infinity $(x, \pm\infty)$ can be established. It can be noted that the presence of a line $(y = 0)$ made up of fixed point leads to have (6) as a structurally unstable map.

Acknowledgments. This work has been performed under the auspices of CNR, Italy, and under the activity of the national research project "Nonlinear Models in Economics and Finance: Complex dynamics, Disequilibrium, Strategic interactions", MIUR, Italy.

REFERENCES

Bischi, G.I & Gardini, L. [1997] "Basin fractalization due to focal points in a class of triangular maps", *International Journal of Bifurcation and Chaos*, vol. 7, No. 7, 1555-1577.

Bischi, G.I & Gardini, L. [1999] "Focal points and basin fractalization in some rational maps", in the *Grazer Mathematische Berichte* (special issue Proceedings ECIT96), Nr.339, pp.61-84.

Bischi G.I. & L. Gardini [2000]. Equilibrium selection and transient dynamics under adaptive and statistical learning, Working Paper n.9, Dip. di Economia Università di Parma.

Bischi, G.I. , L. Gardini & C. Mira [1999] "Maps with denominator. Part I: some generic properties", *International Journal of Bifurcation & Chaos*, vol.9, n.1, 119-153.

Bischi G.I, L. Gardini & C. Mira [2001] "Maps with a vanishing denominator. A survey of some results", *Nonlinear Analysis T.M.&A.* (Special Issue Proceedings of WCNA2000) 47, pp.2171-2185.

Bischi, G.I. , L. Gardini & C. Mira [2003] "Maps with denominator. Part II: noninvertible maps with simple focal points", *International Journal of Bifurcation & Chaos*, in press.

Brock, W.A. & Hommes, C.H. [1997] "A rational route to randomness", *Econometrica*, 65, No. 5, 1059-1095.

Foroni I [2001], Meccanismi di apprendimento in modelli omogenei ed eterogenei, Ph.D. Thesis, University of Trieste.

Gumowski, I. & Mira, C. [1980] *Dynamique Chaotique* (Cepadues Editions, Toulouse).

Marimon R. [1997] "Learning from learning in economic", in D.M. Kreps and k.f. Wallis, eds., *Advances in Economics and Econometrics: Theory and Applications* (Volume I, Cambridge University Press, Cambrifge, UK).

Mira C. [1987] *Chaotic Dynamics. From the one-dimensional endomorphism to the two-dimensional diffeomorphism*. World Scientific, Singapore.

Mira, C., Gardini L., Barugola, A. & Cathala J.C. [1996] *Chaotic dynamics in two-dimensional noninvertible maps* (World Scientific, Singapore).

Laura Gardini
Istituto di Scienze Economiche, University of Urbino
I - 61029 Urbino, Italy
e-mail: *gardini@uniurb.it*

Ilaria Foroni
Dipartimento di Matematica, Università di Milano - Bicocca
I - 20126 Milan, Italy
e-mail: *ilaria.foroni@unimib.it*

Christian Mira
19 rue d'Occitanie,
F - 31130 Quint Fonsegrives, France
and Istituto di Scienze Economiche, University of Urbino
e-mail: *c.mira@free.fr*